Theoretical and Experimental Approaches to Spontaneous Parametric Down Conversion

Sally Steuterman and James Keller
Department of Chemistry, Kenyon College, Gambier, OH

ABSTRACT

In order to further the study of physics at Kenyon, developing an experimental approach to studying quantum phenomena, especially quantum entanglement, is essential. However, in developing the machinery and techniques for studying entanglement, more can be learned than previously thought, not just about entanglement, but also about the best methods for examining quantum phenomena and the effects that come along with them.

INTRODUCTION

Quantum entanglement is a unique occurrence in nature. When two particles become entangled, the states of one reflect upon the other, such that a change in state of one causes an instantaneous reflective change in the other. Though the two particles exist in separate locations in space at one moment in time, it is impossible to describe them as separate entities. Sending the 405 nm pump beam through the BBO crystal creates Type II spontaneous parametric down conversion (SPDC). In Type II SPDC, the idler and signal cones are not coaxial due to the different refractive indices that the cones experience (Fig. 1). Due to the splitting of the cones, several pairs of cones appear. In studying the degenerate case, where both cones are of the same wavelength and therefore are both the size, we can simplify the experimental process. (Fig. 2)

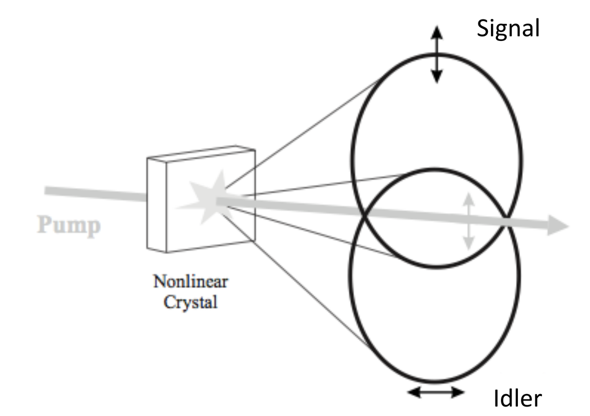

Figure 1: The degenerate cones as formed through the BBO crystal. (Nazirizadeh 2005)

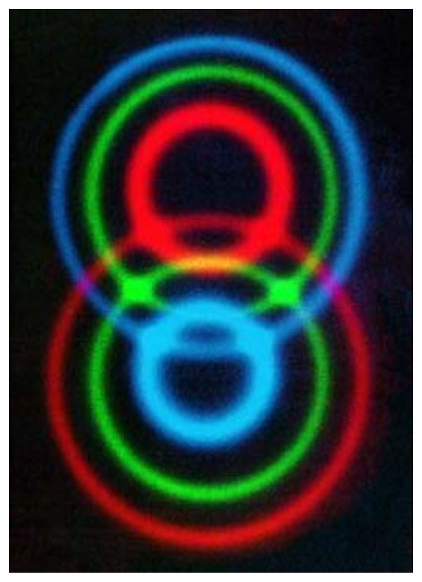

Figure 2: An iconic photo of the cones of excited IR of varying wavelengths (Kwiat 1995).

THE COORDINATE SYSTEM AND THE SIGNAL CONE

As the cones grow larger the intersections between the cones grows farther apart. In order to model the size of the cones, three angles were defined: Θ, off of the optical axis of the crystal, θ, the angle between the projected beam and the pump beam, and Φ, the angle between the projected beam and the beam itself. Calculations were then performed based on the Sellmeier equation as well as the equation for the signal cone (Nazirizadeh 2005). The coordinate system for phase-matching conditions was given by Nazirizadeh (Fig. 3).

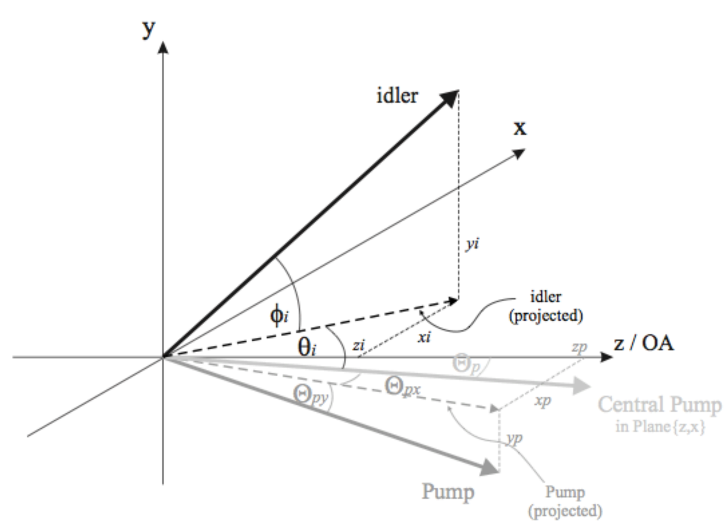

Figure 3: The given coordinate system.

Based off of Nazirizadeh's calculations and assuming Θ_{px} and Θ_{py} are zero, the following equation was entered into Mathematica (Fig. 4):

$$(n_{ep}(\lambda_p,\theta_p)\omega_p y_p - \frac{n_{ei}(\lambda_i)n_{oi}(\lambda_i)\omega_i y_i}{\sqrt{((n_{oi}(\lambda_i))^2+((n_{ei}(\lambda_i))^2-(n_{oi}(\lambda_i))^2)*z_i^2}})^2+(n_{ep}(\lambda_p,\theta_p)\omega_p z_p - \frac{n_{ei}(\lambda_i)n_{oi}(\lambda_i)\omega_i z_i}{\sqrt{((n_{oi}(\lambda_i))^2+((n_{ei}(\lambda_i))^2-(n_{oi}(\lambda_i))^2)*z_i^2}})^2$$
$$+(n_{ep}(\lambda_p,\theta_p)\omega_p x_p - \frac{n_{ei}(\lambda_i)n_{oi}(\lambda_i)\omega_i x_i}{\sqrt{((n_{oi}(\lambda_i))^2+((n_{ei}(\lambda_i))^2-(n_{oi}(\lambda_i))^2)*z_i^2}})^2=(n_{os}(\lambda_s))^2(\omega_p-\omega_i)^2$$

THE IDLER CONE

Solving for the x-component of the idler cone:

$$\omega_i n_{ei}(\lambda_i,\theta_i)x_i+\omega_s n_{os}(\lambda_s)x_s=\omega_p n_{ep}(\lambda_p,\Theta_p)x_p$$
$$x_i=\frac{\omega_p n_{ep}(\lambda_p,\Theta_p)x_p-\omega_s n_{os}(\lambda_s)x_s}{\omega_i n_{ei}(\lambda_i,\theta_i)}$$

Solving for the y-component of the idler cone:

$$\omega_i n_{ei}(\lambda_i,\theta_i)y_i+\omega_s n_{os}(\lambda_s)y_s=\omega_p n_{ep}(\lambda_p,\Theta_p)y_p$$
$$y_i=\frac{\omega_p n_{ep}(\lambda_p,\Theta_p)y_p-\omega_s n_{os}(\lambda_s)y_s}{\omega_i n_{ei}(\lambda_i,\theta_i)}$$

Solving for the z-component of the idler cone:

$$\omega_i n_{ei}(\lambda_i,\theta_i)z_i+\omega_s n_{os}(\lambda_s)z_s=\omega_p n_{ep}(\lambda_p,\Theta_p)z_p$$
$$z_i=\frac{\omega_p n_{ep}(\lambda_p,\Theta_p)z_p-\omega_s n_{os}(\lambda_s)z_s}{\omega_i n_{ei}(\lambda_i,\theta_i)}$$

Normalization of the vectors: $x^2+y^2+z^2=1$

Substitutions based on the coordinate system used:

$$y_p=0$$
$$y_s=\sin(\phi)$$
$$x_p=\sqrt{1-z_p^2}$$
$$z_p=\cos(\Theta_p)$$
$$z_s=\cos(\Theta_p-\theta_s)\sqrt{1-y_s^2}$$
$$x_s=\sqrt{1-y_s^2-z_s^2}$$
$$n_{ep}(\lambda_p,\Theta_p)=\frac{n_{ep}(\lambda_p)n_{op}(\lambda_p)}{\sqrt{(n_{op}(\lambda_p))^2+((n_{ep}(\lambda_p))^2-(n_{op}(\lambda_p))^2)(\cos(\Theta_p))^2}}$$

Based on these substitutions, the final formula entered into Mathematica was (Fig. 5):

$$\frac{(\omega_p n_{ep}(\lambda_p,\Theta_p)x_p-\omega_s n_{os}(\lambda_s)x_s)^2+(\omega_p n_{ep}(\lambda_p,\Theta_p)y_p-\omega_s n_{os}(\lambda_s)y_s)^2+(\omega_p n_{ep}(\lambda_p,\Theta_p)z_p-\omega_s n_{os}(\lambda_s)z_s)^2}{\frac{n_{oi}(\lambda_i)n_{ei}(\lambda_i)}{\sqrt{((n_{oi}(\lambda_i))^2+((n_{ei}(\lambda_i))^2-(n_{oi}(\lambda_i))^2)*(\cos(\theta_i-\Theta_p)*(1-(\sin(\phi_i))^2))^2)}}}=(\omega_p-\omega_s)^2$$

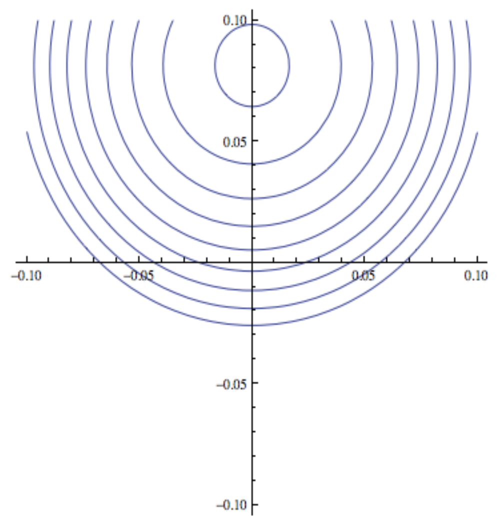

Figure 4. *PhaseMatch-Signal.nb* is the graphical representation of the signal equation.

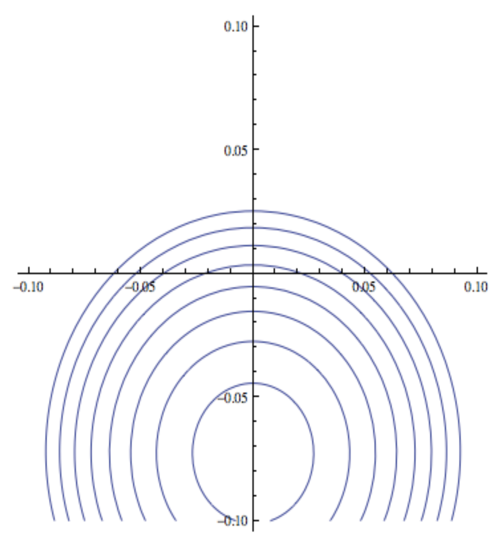

Figure 5. *PhaseMatch-Idler.nb* shows the idler cone to be the reflection of the signal cone over the x-axis as was theorized.

IMAGING

In order for the theories behind the cone size and crystal angle relationship to be confirmed experimentally, images of the infrared cones were taken with a SBIG Instruments ST-8XE model imaging astronomical camera and the contrast was modified using the accompanying CCDOps Software as well as iPhoto to best present the cones. A 10-inch concave lens was placed between the camera and the crystal to slow down the rapid expansion of the cones. Depending on the angle, Θ, that the crystal is tilted at, a combination of two 780 cutoff filters and several high-pass filters in both black and orange were used to cut out and minimize the pump beam.

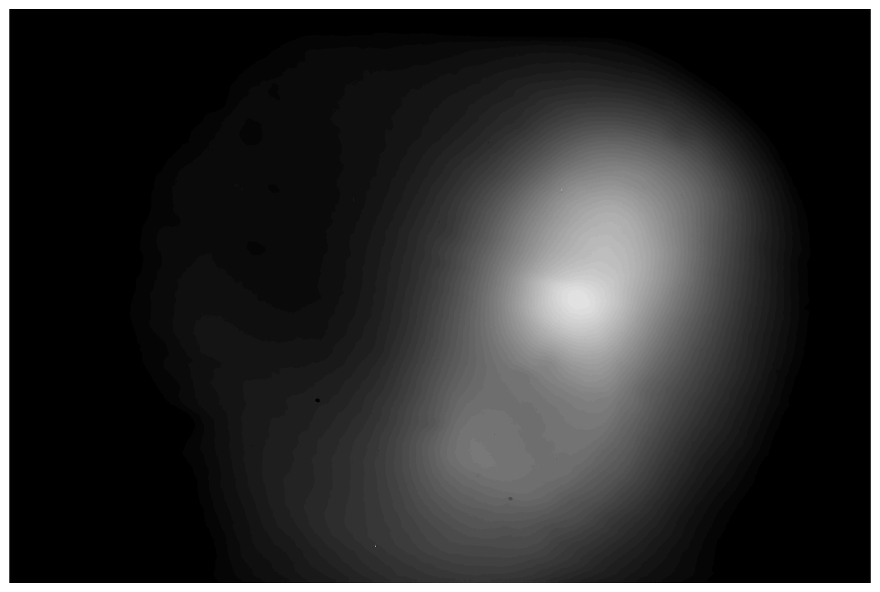

Photo of the two cones with the crystal tilted at 22.75 degrees. This shows the cones to be barely intersecting.

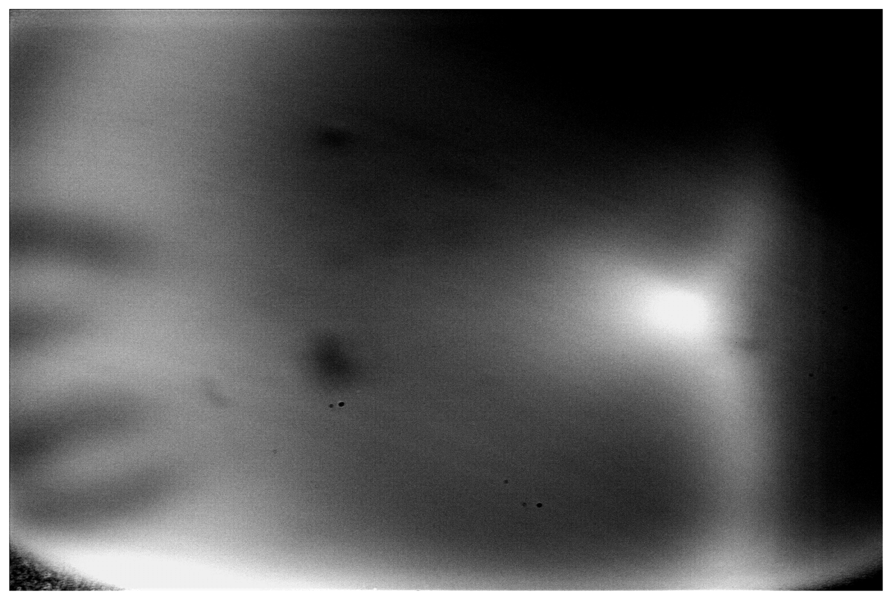

Photo taken of the two cones at 26.000 degrees. 26.000 degrees was shown to be an optimum angle for photon counts (Fine 2011).

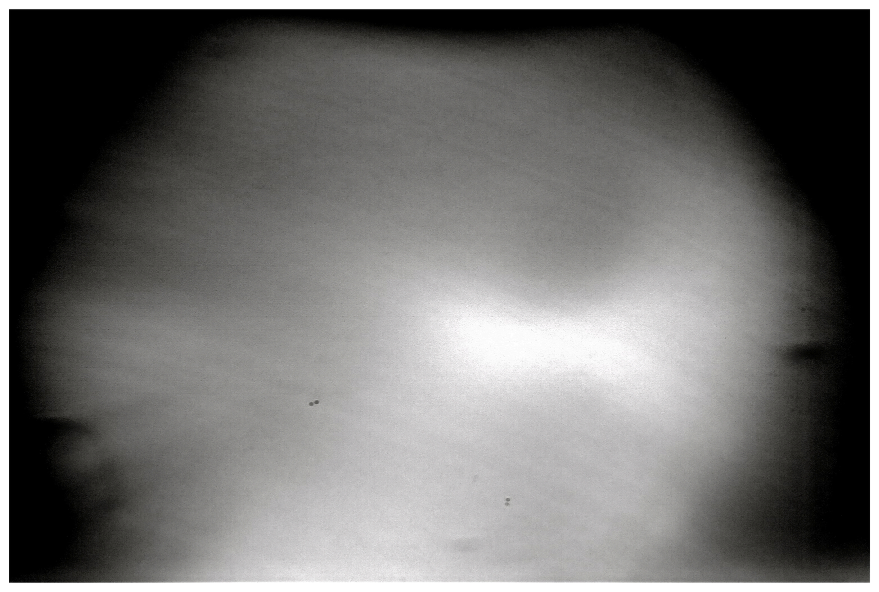

Photo of the two cones taken at 26.00 degrees. The intersections between the two cones are shown to be growing father apart as θ increases.

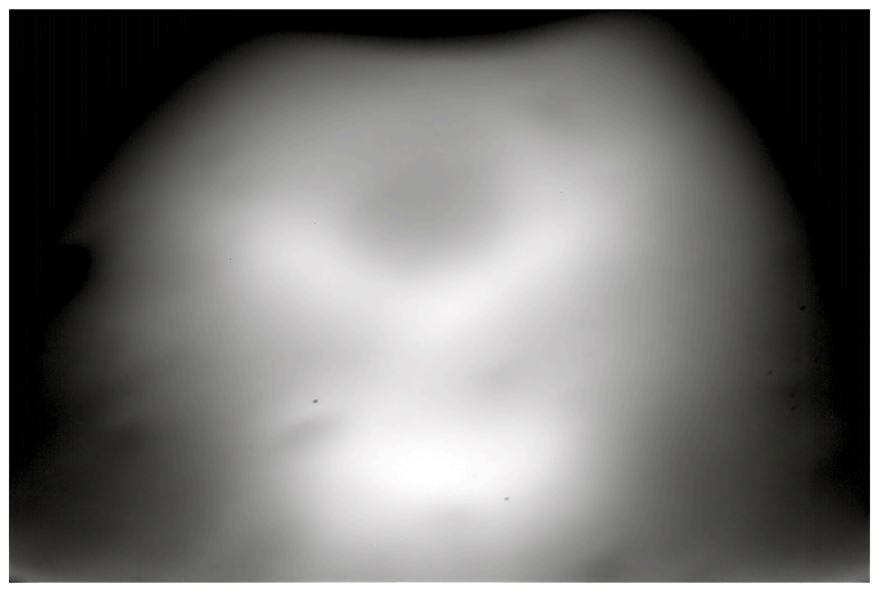

Photo of one of the cones taken with a vertical polarizer with the crystal tilted at 22.56 degrees. This confirms that one of the cones is vertically polarized and the other is horizontally polarized.

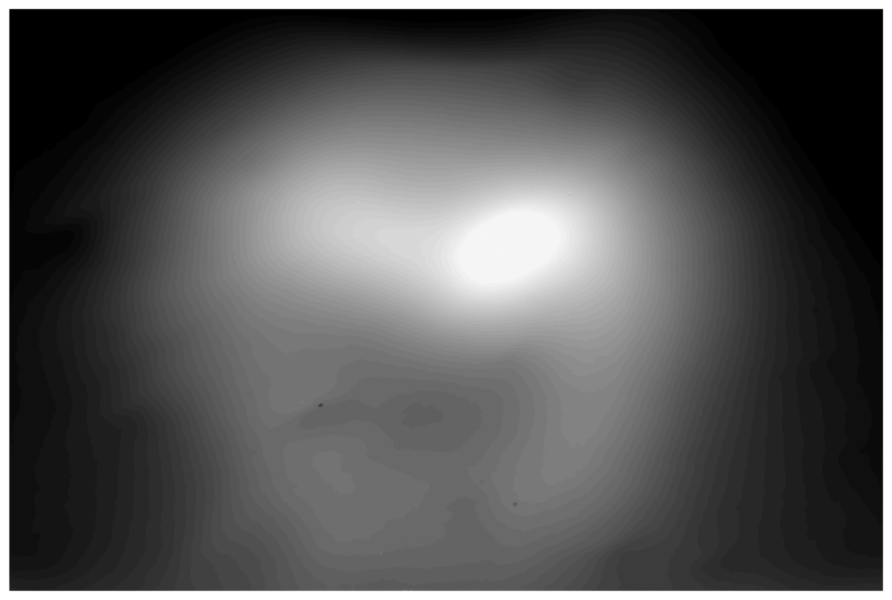

Photo of one of the cones taken with a horizontal polarizer with the crystal tilted at 22.56 degrees. This also serves as confirmation that the two cones have opposite polarizations.

FUTURE WORK

In order to improve the working of the apparatus, the current optics setup should be improved. Ideas that have been shown to improve the operation of the optics to increase the probability of observable entanglement and include the introduction of fiber optics to connect directly to the photon detectors. The more promising thought is to add a large concave mirror behind the crystal to reflect the cones back, which would shorten the setup considerably making it more compact and easier to use.

ACKNOWLEDGEMENTS

Many thanks to Professor Keller for his guidance throughout this project as well as Professor Schumacher for his advice. I would also like to thank the Kenyon College Summer Science Scholars Program.

REFERENCES

Fine, Robert "Quantum State Tomography using Polarization Entangled Photons for the Undergraduate Laboratory" 2012
Nazirizadeh, Yousef "Compact Source for Polarization Entangled Photon Pairs" 2005
Kwiat, P.G. and Reck, M. "New High-Intensity Source for Polarization-Entangled Photon Pairs" *Physics Review* 1995: 75 4337-4341.